Available online at www.sciencedirect.com

ScienceDirect

IFAC Papers Online CONFERENCE PAPER ARCHIVE

IFAC PapersOnLine 56-2 (2023) 7790–7795

Distributed-parameter Bouc-Wen modeling and output feedback control of a piezoactuator for a manipulation task

Sergio Trejo *,** **Gerardo Flores** * **Micky Rakotondrabe** **

* *Laboratorio de Percepción y Robótica [LAPyR], Center for Research in Optics, León, Guanajuato, Mexico*

** *National School of Eng in Tarbes (ENIT), Univ of Toulouse, France*

e-mails: sergiotrejo@cio.mx, gflores@cio.mx, mrakoton@enit.fr

Abstract: The Bouc-Wen hysteresis model and an Euler-Bernouilli beam bending theory are extended to distributed parameter model for a piezoelectric actuator (piezo actuator). Then we use the separation principle for its control and two types of observers: a neural network-based observer and a high-gain observer. Simulations with various conditions show that better performances are obtained when using the neural network-based observer.

Keywords: Bouc-Wen hysteresis model, piezoelectric actuator, observer, control

1. INTRODUCTION

Piezoactuators play an essential role in high-precision and high-speed positioning applications. Indeed they feature high resolution, high bandwidth, and ease of integration[1]. E.g., they are used in microscopy, dental machines, fuel injectors, and robotic hands. Meanwhile, piezoactuators are known to exhibit hysteresis nonlinearity which inevitably degrades the overall performance if not controlled.

Various works are available for the control of piezoactuators to reduce the hysteresis effects. They are categorized as feedback and feedforward architectures. To ensure robustness against uncertainties and external disturbances, feedback architecture is definitely recommended as long as sensor implementation is possible. In the literature, feedback controllers are designed with or without the hysteresis model. The model-based controller design is slightly complex but can account for the specificity of the hysteresis behavior (strength, symmetry, asymmetry,...). Prandtl-Ishlinskii, Preisach, Dahl, and Bouc-Wen [2, 3, 4] hysteresis modeling approaches were the most used for that. Specifically, the Bouc-Wen approach features a structured simplicity (differential model with few parameters) which is well-appropriate for analysis and synthesis. Recently, the classical Bouc-Wen model[5] was used to design a robust output feedback controller valid for symmetrical hysteresis only. Further, the generalized Bouc-Wen model was used to design model predictive control[6] and then a finite time stabilization controller [7] in order to successfully account for the asymmetry of the hysteresis. In all these works, it was assumed that the output displacement was measured, allowing the feedback implementation easily.

This paper is concerned with a piezoactuator displacement control. However, such interested displacement differs from the measured displacement, resulting in a challenging problem. Fig.1 displays the actuator, which has a cantilever structure of length L at which the sensor measures the bending (displacement y_L). However, the displacement y to be controlled is at a distance $x \neq L$ from the clamping. This situation is particularly observed in robotic hand applications: the sensor cannot be placed at the point of interest where the manipulated object is located. Consequently, a model that relates the two displacements y_L and $y = y(x)$ is necessary such that the measurement y_L can be used to control y. The first contribution of the paper

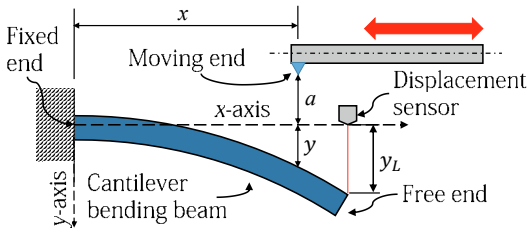

Fig. 1. The system: y is to be controlled to a desirable input y_r, x is distance from clamping, L is beam length, a is a clearance. Available signals are u and y_l.

consists in extending the classical Bouc-Wen model of previous literature to provide the displacement (bending) of the actuator of Fig.1 at any distance from its clamping. The provided distributed parameter (DP) model allows using the measured displacement y_L as feedback control for y. The paper's second contribution is the design of a robust output feedback controller to ensure the stability of the nonlinear system. Two observers are proposed to estimate the states: a high gain observer (HGO),[8], and a neural network observer (NNO),[9]. Several simulations under various conditions demonstrate the better performances obtained from the NNO and the feedback control.

⋆ This work is partially supported by the French - Occitanie region CPER ECOSYSPRO project and IDEA GTO from the Guanajuato Government in Mexico.

10.1016/j.ifacol.2023.10.1154

2. PROBLEM FORMULATION

In [10], the model of the piezoactuator of Fig.1 when we consider the bending at the cantilever tip as the output is:

$$\dot{\mathbf{y}}(t) = A\mathbf{y}(t) + Bv(t) + \delta_y(t) \quad (1)$$

$$v(t) = d_p u(t) - h(t) \quad (2)$$

$$\dot{h}(t) = A_{bw}\dot{u}(t) - B_{bw}|\dot{u}(t)|h(t) - \Gamma_{bw}\dot{u}(t)|h(t)| + \delta_h(t) \quad (3)$$

$$y(t) = C\mathbf{y}(t) \quad (4)$$

In this model, we have:
- $\mathbf{y}$ is an internal state described by realization (A, B, C),
- v is an intermediary signal (output of the nonlinear part),
- u is the driving voltage and input of the system,
- h is an internal state of the hysteresis
- y is the output displacement.

This model has a Hammerstein form (nonlinear static followed by linear dynamics) where the nonlinearity is a classical Bouc-Wen hysteresis model defined by(2) and (3) parameter d_p being an approximated slope for the hysteresis and A_{bw}, B_{bw} and Γ_{bw} indicating its strengh and shape. Last, δ_y and δ_h are perturbations we introduce.

Remind that at low frequency and steady-state conditions, the hysteresis is the only phenomenon observed whilst the dynamics are not. Hence, the classical Bouc-Wen nonlinearity is the static gain of the entire model. As a consequence, the linear dynamics of the Hammerstein form should have unitary gain, i.e. $CA^{-1}B = I$ and $y = v = y_L$.

Our problem is to stabilize bending $y(x,t)$ at distance $x \neq L$ from the clamping to a desired $y_r(t)$. The available information is the distance x, the input control u, and the measurement y_L at the tip. On the other hand, we will consider a feedback control law that requires the state $\mathbf{y}$ and the hysteresis state h which we will be estimated.

3. MODELING EXTENSION

Let us extend the classical Bouc-Wen non-linearity given by (2) and (3) into a x-dependent non-linearity.

3.1 Distributed-parameter linear static model

Considering Euler-Bernoulli bending theory, under the linear and steady-state assumption, the bending of the piezoactuator of Fig.1 at any distance x from the clamping is [11]:

$$y(x) = \frac{m_{piezo}x^2}{2c}u \quad (5)$$

where quantity m_{piezo} is called piezoelectric moment and is based on the physical and geometrical properties of the actuator, while quantity c is its total flexural rigidity.

3.2 Distributed-parameter (DP) nonlinear static model

Assumption 1. For the piezoactuator of length L and for each position x we assume that

$$x \in [0, L], \qquad \dot{x} = 0$$

Proposition 1. The DP classical Bouc-Wen model is obtained by reformulating (3) and (2) according to

$$v_d(x,t) = d_d(x)u(t) - h_d(x,t) \quad (6)$$

$$\dot{h}_d(x,t) = A_d(x)\dot{u}(t) - B_d(x)|\dot{u}(t)|h_d(t) - \Gamma_d(x)\dot{u}(t)|h_d(t)| \quad (7)$$

where the parameters $A_d(x)$, $B_d(x)$, $\Gamma_d(x)$ and $d_d(x)$ are the coefficients of (2) and (3) re-scaled by $(\frac{x}{L})^2$

Proof. Since for the moment, we are not considering the linear part, then $v = y$ applies, $v_d(x,t) = v(t)(\frac{x}{L})^2$ applies to the nonlinear function $h(t)$ by the distributive property, then (7) is obtained from the partial differential equation

$$\frac{\mathrm{d}h_d(x,h)}{\mathrm{d}t} = \frac{\partial h_d}{\partial x}\frac{\mathrm{d}x}{\mathrm{d}t} + \frac{\partial h_d}{\partial h}\frac{\mathrm{d}h}{\mathrm{d}t} + \frac{\partial h_d}{\partial t} \quad (8)$$

where the left term is going to be canceled if we consider the Assumption 1. Evaluating (6) in the boundary condition $y(x = 0, t) = 0$ means a measurement in the base of the beam where there is no variation in y; evaluating in $y(x = L, t) = d_p u(t) - h(\dot{u}, h)$ leads to the model of the beam with Bouc-Wen hysteresis measured at the tip of the beam similar to (2) and (3); and initial condition $y(x, 0)$ is equivalent to the Euler-Bernoulli model(5).

4. OUTPUT FEEDBACK CONTROL

Let Fig.2 show the proposed control scheme for the actuator. In this, two observers will be included and compared. First, a control law using a high gain observer (HGO) [12, 13, 14], and then the same control law but with a neural network observer (NNO) designed to learn the hysteresis behavior.

4.1 High gain nonlinear observer

Since the state h_d is not available, an HGO is used to estimate it. We start by studying the observability of the nonlinear system in a similar way to [12]. Then it will be used as a virtual control input to stabilize $\mathbf{y}$ to the desired value y_r.

Lemma 2. Let us assume that $B \neq 0$, thus the system (1), (6), and (7) is observable.

Proof. We can arrange the system given by (1), (6), and (7) as

$$\begin{aligned} \dot{\mathbf{z}} &= \Gamma\mathbf{z} + g(\mathbf{z}, \mathbf{v}) + \delta(t) \\ \mathbf{y} &= \bar{C}\mathbf{z} \end{aligned} \quad (9)$$

where $\mathbf{z} = [\mathbf{y}, h_d]^T$ is the state vector, $\mathbf{v} = [x, u, \dot{u}]^T$ is the input vector, $\mathbf{y}$ is the output vector, where we have chosen $\mathbf{y} = y_d = (x/L)^2 y_L$ for simplicity, $\Gamma = \begin{pmatrix} 0 & -B \\ 0 & 0 \end{pmatrix}$, $g(\mathbf{z}, \mathbf{v}) = [A\mathbf{y} + Bd_d u, f(x, \dot{u}, h_d)]^T$ is a nonlinear function, $f(x, \dot{u}, h_d) = \dot{h}_d$, and $\bar{C} = [1, 0]$.

If the observability matrix is $O = [\bar{C}, \bar{C}\Gamma]^T$ and $B \neq 0$ it is full rank, then the system (9) is observable. Moreover, the system is uniform since its observability does not depend on its inputs.

For the HGO proposed to control the system (9) we take the following assumptions

Assumption 2. The control input $\mathbf{v}(t)$ and its time-derivative $\dot{\mathbf{v}}(t)$ are bounded.

Assumption 3. The disturbance vector $\delta(t) = [\delta_z, \delta_h]^T$ in (9) is bounded by $\|\delta\| \leq \varrho\|\epsilon\|$, where $\epsilon = \hat{\mathbf{z}} - \mathbf{z}$ is the observation error, and $\varrho \in \mathbb{R}^+$.

Proposition 3. Considering Assumptions 2 and 3 the observer that globally exponentially stabilizes the origin $\epsilon = \hat{\mathbf{z}} - \mathbf{z}$ proposed is

$$\dot{\hat{\mathbf{z}}} = \Gamma\hat{\mathbf{z}} + g(\hat{\mathbf{z}}, \mathbf{v}) - S^{-1}\bar{C}^T(\hat{\mathbf{y}} - \mathbf{y}) \tag{10}$$

where S is the solution of

$$\theta S + \Gamma^T S + S\Gamma - \bar{C}^T\bar{C} = 0 \tag{11}$$

Proof. The solution of (11) is $S = \begin{pmatrix} 1/\theta & B/\theta^2 \\ B/\theta^2 & 2B^2/\theta^3 \end{pmatrix}$ which is a symmetric positive definite matrix for $\theta \in \mathbb{R}^+$. Then we can set the time derivative of the error $\epsilon = \hat{\mathbf{z}} - \mathbf{z}$ as

$$\dot{\epsilon} = (\Gamma - S^{-1}\bar{C}^T\bar{C})\epsilon + g(\hat{\mathbf{z}}, \mathbf{v}) - g(\mathbf{z}, \mathbf{v}) - \delta(t) \tag{12}$$

The Lyapunov function we use is $V_o = \epsilon^T S\epsilon$ whose time-derivative along solutions of system (9) and HGO (10) gives

$$\dot{V}_o = 2\epsilon^T(S\Gamma - \bar{C}^T\bar{C})\epsilon + 2\epsilon^T S(g(\hat{\mathbf{z}}, \mathbf{v}) - g(\mathbf{z}, \mathbf{v}) - \delta(t)). \tag{13}$$

Combining (13), (11) and Assumption 2 we have

$$\begin{aligned}\dot{V}_o = -2\epsilon^T(\theta S + \Gamma^T S)\epsilon + 2\|\epsilon\|\|S\|\|g(\hat{\mathbf{z}}, \mathbf{v}) - g(\mathbf{z}, \mathbf{v})\| \\ +2\|\epsilon\|\|S\|\|\delta(t)\|.\end{aligned} \tag{14}$$

Since $S\Gamma - \bar{C}^T\bar{C} = -\theta S - \Gamma^T S$ is negative definite by(11), assuming the global Lipschitz condition applies $\|g(\hat{\mathbf{z}}, \mathbf{v}) - g(\mathbf{z}, \mathbf{v})\| \leq l_g\|\hat{\mathbf{z}} - \mathbf{z}\|$ and the Assumption 3 as well

$$\dot{V}_o \leq -\theta\epsilon^T S\epsilon + 2l_g\|\epsilon\|^2\|S\| + 2\varrho\|\epsilon\|^2\|S\| \tag{15}$$

it follows that $\dot{V}_o \leq -(\theta - 2l_g - 2\varrho)V_o$. Then since V_o is radially unbounded, the equilibrium point ϵ is globally exponentially stable as long as $\theta > 2(l_g + \varrho)$.

4.2 Control for the linear dynamics

Now that the state $\hat{\dot{\mathbf{z}}} = [\hat{\dot{y}}, \hat{\dot{h}}_d]^T$ is estimated, we can use it to control the system (9). Using the separation principle [15, 16], the approach is shown in Fig.2. The first stage uses the reference signal h_{dr} as a virtual control since, in the DPM, h_d represents an exogenous signal. This allows designing the control that outputs the control variable u. To this, we use the following assumptions:

Assumption 4. The system's individual disturbances are bounded as follows:

$$|\delta_y| \leq \varrho_1|e_{\mathbf{y}}|, \qquad |\delta_h| \leq \varrho_2|e_h|$$

where $e_{\mathbf{y}} = \hat{\mathbf{y}} - \mathbf{y}_r$ and $e_h = \hat{h}_d - h_{dr}$.

Proposition 4. The virtual control that globally asymptotically stabilizes $e_{\mathbf{y}} = 0$, if $\kappa_1 > \varrho_1$, and $|\delta_y| \leq \varrho_1|e_{\mathbf{y}}|$ holds.

$$h_{dr} = \frac{1}{B}([A + \kappa_1]e_{\mathbf{y}} + A\mathbf{y}_r - \dot{\mathbf{y}}_r + Bd_p u) \tag{16}$$

Proof. Let us propose the Lyapunov function $V_y = \frac{1}{2}e_{\mathbf{y}}^2$ and its time-derivative $V_y = e_{\mathbf{y}}\dot{e_{\mathbf{y}}}$ with equation (1)

$$\dot{V}_y = e_{\mathbf{y}}(A[e_{\mathbf{y}} + \mathbf{y}_r] + Bd_d u - Bh_d + \delta_y(t) - \dot{\mathbf{y}}_r) \tag{17}$$

If we substitute the virtual control (16) assuming that $e_h \to 0$ in (7), after Assumptions 2 and 4, we obtain

$$\begin{aligned}\dot{V}_y = e_{\mathbf{y}}\Big(Ae_{\mathbf{y}} + A\mathbf{y}_r + Bd_d u + \delta_y(t) \\ -B\big(\frac{1}{B}([A + \kappa_1]e_{\mathbf{y}} + A\mathbf{y}_r - \dot{\mathbf{y}}_r + Bd_d u)\big) - \dot{\mathbf{y}}_r\Big) \\ \leq -\kappa_1 e_{\mathbf{y}}^2 + \varrho_1|e_{\mathbf{y}}|^2 \leq -(\kappa_1 - \varrho_1)e_{\mathbf{y}}^2\end{aligned} \tag{18}$$

consequently, the closed-loop system is globally exponentially stable given that $B \neq 0$.

4.3 Control for the nonlinear subsystem

The second stage stabilizes the nonlinear behavior generating the control u by solving the tracking problem, i.e. by finding u such that h_d converges to the virtual control h_{dr}. Since we already have h_d, we use it as input to the nonlinear system to generate the input signal u for the system. First, we take into account the following assumption

Assumption 5. The desired signal h_{dr} and $\dot{h}_{dr}$ are bounded as follows,

$$|h_{dr}| \leq c_1, \qquad |\dot{h}_{dr}| \leq c_2|e_h|$$

with $c_1, c_2 \in \mathbb{R}^+$, where $e_h = \hat{h}_d - h_{d_r}$.

Proposition 5. If we consider Assumption 5 and Assumption 4, the proposed control that locally exponentially stabilizes the nonlinear subsystem is

$$\dot{u} = \frac{1}{A_d}\Big(k_1 \operatorname{sgn}(e_h)\sqrt{|e_h|} + k_2 e_h\Big). \tag{19}$$

Proof. Let us define the error dynamics as follows

$$\dot{e_h} = \dot{u}(A_d - \Gamma_d|e_h + h_d|) - B_d|\dot{u}|(e_h + h_d) + \delta_h(t) - \dot{h}_{d_r} \tag{20}$$

Considering the Lyapunov function $V_c = |e|$ and its time derivative taking into account the dynamics of error

$$\begin{aligned}\dot{V}_c &= \operatorname{sgn}(e_h)(\dot{u}(A_d - \Gamma_d|e_h + h_{dr}|) \\ &\quad - B_d|\dot{u}|(e_h + h_{dr}) + \delta_h(t) - \dot{h}_{dr}) \\ &\leq k_1\sqrt{|e_h|} + k_2|e_h| + (|\Gamma_d| + |B_d|)|\dot{u}|(|e_h| + |h_{dr}|) \\ &\quad + |\delta_h| + |\dot{h}_{dr}|\end{aligned} \tag{21}$$

Considering the Assumptions 4 and 5, and that $|\dot{u}| \leq \frac{1}{|A_d|}(k_1\sqrt{|e_h|} + k_2|e_h|)$ and $k_1\sqrt{|e_h|} + k_2|e_h| \leq \alpha\sqrt{|e_h|}$

$$\begin{aligned}\dot{V}_c \leq -(-k_1 - \frac{c_1\alpha}{|A_d|}(|\Gamma_d| + |B_d|)\sqrt{|e_h|} \\ -(-k_2 + \varrho_2 + c_2)|e_h| + \frac{\alpha}{|A_d|}(|\Gamma_d| + |B_d|)\sqrt{|e_h|}|e_h|\end{aligned} \tag{22}$$

then

$$\dot{V}_c \leq -\beta|e_h| + \rho\sqrt{|e_h|}|e_h| - \sigma\sqrt{|e_h|} \tag{23}$$

where

$$\begin{aligned}\rho = \frac{\alpha}{|A_d|}(|\Gamma_d| + |B_d|), \\ \beta = -k_2 - \varrho_2 - c_2, \sigma = -k_1 - c_1\rho,\end{aligned} \tag{24}$$

are chosen as positive real numbers such that the solution of $\dot{V}_c \leq 0$ when

$$|e_h| \leq \min\left\{\Big(\frac{\alpha - k_1}{k_2}\Big)^2, \frac{\beta\sqrt{4\sigma\rho + \beta^2} + 2\sigma\rho + \beta^2}{2\rho^2}\right\} \tag{25}$$

Then the equilibrium point $e_h = 0$ locally exponentially stabilizes (7).

Remark 1 The virtual control (16) could work using the available signal or the estimated signal from the observer.

4.4 Neural Network observer

The NNO aims to obtain estimated states employing a neural network and a regular observer. The feedforward

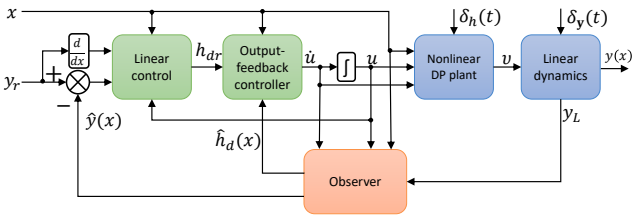

Fig. 2. The control system where y is to be controlled to a desired y_r, and x is an input parameter

neural network is used to parameterize the nonlinearities of the hysteresis of the system, i.e., the function $\hat{g}(\hat{\mathbf{z}}, \mathbf{v}) = \dot{h}$, using the only measurable state $\dot{\mathbf{y}}$ for training by back-propagation algorithm. For the case we addressed here, we cannot train using the whole state $\dot{\mathbf{z}}$ since the hysteresis variable h is not available for measurement. The function $\hat{g}(\hat{\mathbf{z}}, \mathbf{v})$ by itself is useful for plugging it in other controllers where the term $\dot{h}$ is employed, and for different devices as well.

We must consider a nonlinear continuous-time system like

$$\dot{\mathbf{z}} = \Gamma \mathbf{z} + g(\mathbf{z}, \mathbf{v}) \tag{26}$$

$$\mathbf{y} = C\mathbf{z} \tag{27}$$

where $\mathbf{z} \in \mathbb{R}^n$, $\mathbf{y} \in \mathbb{R}^l$, $\mathbf{v} \in \mathbb{R}^m$, $g(z, v) = f(z, v) - \Gamma \mathbf{z}$ and the pair (C, Γ) is observable. We can describe the state observer of the system with

$$\begin{aligned} \dot{\hat{\mathbf{z}}} &= \Gamma \hat{\mathbf{z}} + \hat{g}(\hat{\mathbf{z}}, \mathbf{v}) + G(y - C\hat{\mathbf{z}}) \\ \hat{\mathbf{y}} &= C\hat{\mathbf{z}} \end{aligned} \tag{28}$$

where $\hat{\mathbf{z}}$ is the state and $\hat{\mathbf{y}}$ is the output of the observer, the observer gain $G \in \mathbb{R}^{n \times l}$ is selected such that $\Gamma - GC$ is a Hurwitz matrix. Since Γ is selected such that (C, Γ) is observable, then G exists. It was already shown [17] that for enough large number of neurons, there exist weights and thresholds such that any continuous function can be represented as

$$g(\mathbf{z}, \mathbf{v}) = W\sigma(V\bar{z}) + \epsilon(\mathbf{z}) \tag{29}$$

where $W \in \mathbb{R}^{n \times k}$ is the weight matrix of the output and $V \in \mathbb{R}^{k \times (n+m)}$ the matrices of the hidden layers, k is the number of hidden neurons, $\bar{z} = [\mathbf{z}, \mathbf{v}]$, is the input of the NN, $\epsilon(\mathbf{z})$ is the approximation error, and $\sigma(.)$ is the sigmoidal activation function of the hidden neurons. The sigmoidal function is $\sigma_i(V_i\bar{z}) = \frac{2}{1+e^{-2V_i\bar{z}}} - 1$, where V_i is the ith row of V, and $\sigma_i(V_i\bar{z})$ is the ith element of $\sigma(V\bar{z})$.

Assumption 6. The upper bound on fixed ideal weights W, V and σ exists such that

$$\|W\|_F \leq W_M, \quad \|V\|_F \leq V_M, \quad \|\sigma(V\bar{z})\| \leq \sigma_m$$

Then we have function g approximated by

$$\hat{g}(\hat{\mathbf{z}}, \mathbf{v}) = \hat{W}\sigma(\hat{V}\hat{\bar{z}}) \tag{30}$$

Consider the model given in (44)-(45) and (30), the NNO is given by

$$\begin{aligned} \dot{\hat{\mathbf{z}}} &= \Gamma \hat{\mathbf{z}} + \hat{W}\sigma(\hat{V}\hat{\bar{z}}) + G(\mathbf{y} - \hat{\mathbf{y}}) \\ \hat{\mathbf{y}} &= C\hat{\mathbf{z}} \end{aligned} \tag{31}$$

If we define the state estimation error $e_{\mathbf{z}} = \bar{z} - \hat{\bar{z}}$ and output estimation error $e_{\mathbf{y}} = \bar{y} - \hat{\bar{y}}$, consider(30) and subtract (31) from (28), the error dynamics is expressed

$$\begin{aligned} \dot{e_{\mathbf{z}}} &= \Gamma \mathbf{z} + W\sigma(V\bar{z}) - \Gamma\hat{\mathbf{z}} - \hat{W}\sigma(\hat{V}\hat{\bar{z}}) - Ge_{\mathbf{y}} + \epsilon(\mathbf{z}) \\ &= \Gamma_c e_{\mathbf{z}} + e_w\sigma(e_v\hat{\bar{z}}) + w(\mathbf{z}) \end{aligned} \tag{32}$$

where $e_W = W - \hat{W}$, $e_V = V - \hat{V}$, $\Gamma_c = \Gamma - GC$, $w(t) = W[\sigma(V\bar{z}) - \sigma(\hat{V}\hat{\bar{z}})]$ is bounded as $\|w(t)\| \leq \bar{w}$ for some positive constant $\bar{w}$, due to the sigmoidal function and the boundedness of the ideal neural network weights. The eigenvalues of Γ_c are farther to the left in the complex plane than the eigenvalues of Γ, helping the states of the estimator to track the states of the actual system with more accuracy.

Proposition 6. Consider the system (9) and the observer dynamics (32), if the weights are modified with the tuning algorithm given by the equations

$$\begin{aligned} \dot{\hat{W}} &= -\eta_1(e_{\mathbf{y}}^T C\Gamma_c^{-1})^T\sigma^T(\hat{V}\hat{\bar{z}}) - \rho_1\|e_{\mathbf{y}}\|\hat{W} \\ \dot{\hat{V}} &= -\eta_2(e_{\mathbf{y}}^T C\Gamma_c^{-1}\hat{W}(I - \Lambda(\hat{V}\hat{\bar{z}}))^T \operatorname{sgn}(\hat{\bar{z}})^T - \rho_2\|e_{\mathbf{y}}\|\hat{V} \end{aligned} \tag{33}$$

where $\Lambda(\hat{V}\hat{\bar{z}}) = diag\{\sigma_i^2(\hat{V}\hat{\bar{z}}\}$, $i = 1, 2, ..., m$, $sign(.)$ is the sign function, the learning rates $\eta_1, \eta_2 > 0$, ρ_1, ρ_2 are small positive numbers, then the state estimation error $e_{\mathbf{z}}$, and weight estimation errors e_V and e_V are uniformly ultimately bounded.

Proof. In (33), the first terms are back-propagation terms, and the second terms are the e-modification terms for incorporating damping in the equations and the details of its proof are in [18].

We must consider the positive definite Lyapunov function candidate $V_n = \frac{1}{2}e_{\mathbf{z}}^T P e_{\mathbf{z}} + \frac{1}{2}\operatorname{Tr}(e_W^T e_W) + \frac{1}{2}\operatorname{Tr}(e_V^T e_V)$ where $P = P^T$ is a positive-definite matrix that satisfies $\Gamma_c^T P + P^T\Gamma_c = -Q$ for a positive definite matrix Q. The time derivative of V_n is

$$\dot{V}_n = \frac{1}{2}\dot{e}_{\mathbf{z}}^T P e_{\mathbf{z}} + \frac{1}{2}e_{\mathbf{z}}^T P\dot{e}_{\mathbf{z}} + \frac{1}{2}\operatorname{Tr}(e_W^T\dot{e}_W) + \frac{1}{2}\operatorname{Tr}(e_V^T\dot{e}_V) \tag{34}$$

The learning rules (33) written as functions of e_W and e_V are

$$\begin{aligned} \dot{e_W} &= \eta_1(e_{\mathbf{y}}^T C\Gamma_c^{-1})^T\sigma^T(\hat{V}\hat{\bar{z}}) + \rho_1\|e_{\mathbf{y}}\|\hat{W} \\ \dot{e_V} &= \eta_2(e_{\mathbf{y}}^T C\Gamma_c^{-1}\hat{W}(I - \Lambda(\hat{V}\hat{\bar{z}}))^T \operatorname{sgn}(\hat{\bar{z}})^T + \rho_2\|e_{\mathbf{y}}\|\hat{V} \end{aligned} \tag{35}$$

Substituting $\Gamma_c^T P + P^T\Gamma_c = -Q$ and then equations (32), (33) and (35) into (34) we have

$$\begin{aligned} \dot{V}_n = &-\frac{1}{2}e_{\mathbf{z}}^T Q e_{\mathbf{z}} + e_{\mathbf{z}}^T P(e_W\sigma(\hat{V}\hat{\bar{z}}) + w) \\ &+ \operatorname{Tr}(e_W^T l_1 e_{\mathbf{z}}\sigma^T(\hat{V}\hat{\bar{z}}) - e_W^T\rho_1\|Ce_{\mathbf{z}}\|(W - e_W)) \\ &+ \operatorname{Tr}(e_V^T(I - \Lambda(\hat{V}\hat{\bar{z}}))^T\hat{W}l_2 e_{\mathbf{z}}\operatorname{sgn}^T(\hat{\bar{z}})) \\ &+ e_W^T\rho_2\|Ce_{\mathbf{z}}\|(V - e_V)) \end{aligned} \tag{36}$$

where $l_1 = \eta_1\Gamma_c^{-T}C^T C$, $l_2 = \eta_2\Gamma_c^{-T}C^T C$. We can obtain with the help of Assumption 6 the following inequalities

$$\begin{aligned} \operatorname{Tr}(e_W^T(W - e_W)) &\leq W_M\|e_W\| - \|e_W\|^2 \\ \operatorname{Tr}(e_V^T(V - e_V)) &\leq V_M\|e_V\| - \|e_V\|^2 \\ \operatorname{Tr}(e_W^T l_1 e_{\mathbf{z}}\sigma^T(\hat{V}\hat{\bar{z}})) &\leq \sigma_m\|e_W^T\|\|l_1\|\|e_{\mathbf{z}}\| \end{aligned} \tag{37}$$

The last equation in (37) uses the property of two column vectors $\operatorname{Tr}(AB^T) = B^T A$. Using this property with $\|\hat{W}\| = \|W - e_W\| \leq W_M + \|e_W\|$, $1 - \sigma_m^2 \leq 1$ gives

$$\begin{aligned} &\operatorname{Tr}(e_V^T(I - \Lambda(\hat{V}\hat{\bar{z}}))^T\hat{W}^T l_2 e_{\mathbf{z}}\operatorname{sgn}^T(\hat{\bar{z}}) \\ &\qquad \leq \|e_V\|(W_M + \|e_W\|)\|l_2\|\|e_{\mathbf{z}}\|. \end{aligned} \tag{38}$$

Substituting inequalities (37) and (38) into (36) we get

$$\dot{V}_n \leq -\frac{1}{2}\lambda_{min}(Q)\|e_{\mathbf{z}}\|^2 + \|e_{\mathbf{z}}\|\|P\|(\|e_W\|\sigma_m + \bar{w}) + \sigma_m\|e_W\|\|l_1\|\|e_{\mathbf{z}}\| + (W_M\|e_W\| - \|e_W\|^2)\rho_1\|C\|\|e_{\mathbf{z}}\| + \|e_V\|\|l_2\|(W_M + \|e_W\|)\|e_{\mathbf{z}}\| + \rho_2\|C\|\|e_{\mathbf{z}}\|(V_M\|e_V\| - \|e_V\|^2) = F \tag{39}$$

where λ_{min} is the minimum eigenvalue of Q. We must ensure the $\dot{V}_n$ is negative by completing the squares of terms involving $\|e_W\|$ and $\|e_V\|$. To this, we try to find some conditions on $\|e_{\mathbf{z}}\|$ despite the weights errors. Firstly we define $K_1 = (\|l_2\|/2)$, then we add and subtract $K_1^2\|e_W\|^2\|e_{\mathbf{z}}\|$ and $\|e_V\|^2\|e_{\mathbf{z}}\|$ to the right side of (39), we have

$$F = -\frac{1}{2}\lambda_{min}(Q)\|e_{\mathbf{z}}\|^2 + \Big[\|P\|\bar{w} - (\rho_1\|C\| - K_1^2)\|e_W\| + \|P\|\sigma_m + \sigma_m\|l_1\| + \rho_1\|C\|W_M)\|e_W\| + (\rho_2\|C\|V_M + \|l_2\|W_M)\|e_V\| + (\rho_2\|C\| - 1)\|e_V\|^2 - (K_1\|e_V\| - \|e_V\|^2)\Big]\|e_{\mathbf{z}}\| \tag{40}$$

If we add and subtract from (40) the terms $K_2^2\|e_{\mathbf{z}}\|$ and $K_3^2\|e_{\mathbf{z}}\|$ where

$$K_2 = \frac{p_1 W_M\|C\| + \sigma_m\|l_1\| + \|P\|\sigma_m}{2(\rho_1\|C\| - K_1^2)}$$

$$K_3 = \frac{p_1\|C\|V_M + \|l_2\|W_M}{2(\rho_2\|C\| - 1)}$$

then we have

$$F = -\frac{1}{2}\lambda_{min}(Q)\|e_{\mathbf{z}}\|^2 + \Big[\|P\|\bar{w} - (\rho_1\|C\| - K_1^2)K_2^2 + (\rho_2\|C\| - 1)K_3^2 - (\rho_1\|C\| - K_1^2)(K_2 - \|e_W\|)^2 - (\rho_2\|C\| - 1) \times (K_3 - \|e_V\|)^2 - (K_1\|e_W\| - \|e_V\|^2)\Big]\|e_{\mathbf{z}}\| \tag{41}$$

Assuming $\rho_1 \geq (K_1^2/\|C\|)$, $\rho_2 \geq (1/\|C\|)$ and considering that the last three terms of (41) are negative

$$F = -\frac{1}{2}\lambda_{min}(Q)\|e_{\mathbf{z}}\|^2 + \|e_{\mathbf{z}}\| \times \big(\|P\|\bar{w} - (\rho_1\|C\| - K_1^2)K_2^2 + (\rho_2\|C\| - 1)K_3^2\big) \tag{42}$$

Therefore, the condition on $\|e_{\mathbf{z}}\|$ guarantees the negative semi-definiteness of $\dot{V}_n$

$$\|e_{\mathbf{z}}\| > \frac{2\big(\|P\|\bar{w} - (\rho_1\|C\| - K_1^2)K_2^2 + (\rho_2\|C\| - 1)K_3^2\big)}{\lambda_{min}(Q)} = b \tag{43}$$

$\dot{V}_n$ is negative definite outside the ball with radius b described as $X = \{e_z|\|e_z\| > b\}$, and e_z is uniformly ultimately bounded, this is, when $\dot{L}$ increases for smaller values of $||\tilde{x}||$ will increase L and $\tilde{x}$, if $\tilde{x}$ goes outside the ball χ where $\dot{L}$ is negative semi-definite and then L and $\tilde{x}$ will be reduced. To achieve more accuracy, b should be smaller, and a proper Γ_c should be selected, the damping factors η_1 and η_2 and learning rates ρ_1 and ρ_2. To adjust the convergence of the neural network, when the learning rates increase, they can lead to a faster convergence, but if it goes too high, we can get overshoot. On the other hand, a higher damping factor improves the system's stability, but too much damping can lead to a non-optimal convergence of weights. The Hurwitz matrix Γ_c should be more stable as the eigenvalues go farther to the left of the complex plane, however, a more stable matrix Γ_c may slow down the convergence of the weights. The best solution normally is a more stable matrix Γ_c for accuracy and higher learning rates to improve the convergence.

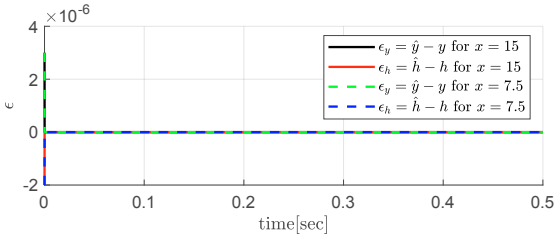

Fig. 3. Tracking error response time with x=15mm and x=7.5mm, frequency 10Hz.

5. SIMULATION

Note that the actuator exhibits the same dynamics whatever the chosen x is. Hence, combining the model given by (1)-(4) with the DP model given by (6) and (7), the final system model is:

$$\dot{\mathbf{y}}(t) = A\mathbf{y}(t) + B\boldsymbol{\upsilon}(t) + \delta_y(t) \tag{44}$$

$$\boldsymbol{\upsilon}(x,t) = \mathbf{d}(x)u(t) - \mathbf{h}(x,t) \tag{45}$$

$$\dot{h}_d(x,t) = A_d(x)\dot{u} - B_d(x)|\dot{u}|h - \Gamma_d(x)\dot{u}|h| + \delta_h(t) \tag{46}$$

$$y(t) = C\mathbf{y}(t) \tag{47}$$

Note that at steady state, we have: $CA^{-1}B = I$ and $y = \upsilon_2(x) = y(x)$. We will take $C = 1$ for the simplicity, $\mathbf{d}(x) = [d_p, d_d]^T$, $\mathbf{h}(x,t) = [h, h_d]^T$, $\boldsymbol{\upsilon}(x,t) = [\upsilon, \upsilon_d]^T$ and $\mathbf{y}(t) = [y_L, y(x)]^T$. The introduced disturbances are $\delta_y = 30\mu m$ and $\delta_h = 25sin(t)\mu m$.

5.1 High gain observer

The units of y_r, y, x and h_d are μm, the input u is in Volts. The parameters considered were experimentally obtained from a piezoactuator made of lead zirconate titanate material and Nickel of total length $L = 20mm$ [10]. The parameters of the classical Bouc-Wen submodel are $d_p = 1.6\mu m/V$, $A_d = 0.9\mu m/V$, $B_d = \Gamma_d = 0.008V^{-1}$, while those of the linear dynamics are $A = 1/\tau$, $B = -1/\tau$ where $\tau = 1ms$. In the simulations the reference input was $\mathbf{y}_r = 80 \times 10^{-6}\sin(2\pi ft)$, where frequency f is $1Hz$, $10Hz$ and $30Hz$. The values of x are fixed at two distances $7.5mm$ and $15mm$. The initial conditions were $[\mathbf{y}, h_d]^T = [3, -2]^T$. The parameters used for the HGO were $\theta = 100$, $k_1 = 2$, $k_2 = 2$, and $\kappa_1 = 4000$.

In Fig.3, the error ϵ of the HGO and state values y and h_d is shown, which is small.

5.2 Training

Since the only available signals for measurement are in the vector $\mathbf{v} = [x, u, y_L]$ we used, in this case, u and fixed x as inputs, and then the label for training is the signal y_L. The training database was generated using the input and output of the system controlled by the high gain observer by sampling x in the points 7.5, 10, 12.5, 15, and 17.5 mm, and the three frequencies $f = 1$, 10, 30 Hz.

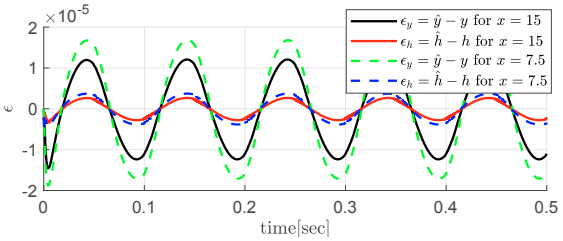

Fig. 4. Reference-Output response time with x=15mm and x=7.5mm, frequency 10Hz.

The weights of the neural network W and V were normally distributed random matrices of size 2×3 and 3×3, respectively. The mean absolute error (MAE) cost function used was $C_{MAE} = \frac{1}{N}\sum_i^N |\hat{\mathbf{z}}_i - \mathbf{z}_i|$ for N number of points in the dataset. The learning rates were $\eta_1 = \eta_2 = 100$ and $\rho_1 = \rho_2 = 1$, $\theta = 200$ in 500 epochs. For simulation, the values of $k_1 = k_2 = 1$ and $\kappa_1 = 4000$ were used, and the other parameters remained unchanged from the NNO and controller.

Fig.4 displays the error ϵ of the observer and state values y and h_d, which is small although the oscillations due to the nature of the neural network as an approximation of the hysteresis, in opposition to NNO which uses the same hysteresis parameters of the system in this case.

6. CONCLUSION

This paper presented the modeling and control of a piezoactuator having a cantilever structure and which exhibited hysteresis non-linearity. Contrary to the existing works where the measured displacement is the same as the displacement to be controlled, the paper considered that they were not collocated. To this, we first proposed a model that expressed the displacement (bending) of the actuator at any distance from its clamping which allowed us to have a relation between the measured displacement with the one to be controlled. The model extends the classical Bouc-Wen model within a Hammerstein structure. Then, two observers - a high gain (HGO) and a neural network (NNO) - were developed for the further output feedback control of the actuator. Finally, several simulations showed that the HGO proposes better performances in spite of noise terms δ_h and δ_y in the system's model. The fairest and most objective comparison would be given with experimental measurements since the neural network would adjust directly to experimental data instead of to a mathematical model. Experimental implementation of the proposed observer and control on a real actuator is planned as perspectives to confront the simulation results.

REFERENCES

[1] M. Rakotondrabe. Smart materials-based actuators at the micro/nano-scale: Characterization, control and applications. *Springer, ISBN 978-1-4614-6683-3*, 2013.

[2] Santosh Devasia, Evangelos Eleftheriou, and SO Reza Moheimani. A survey of control issues in nanopositioning. *IEEE Trans on Control Systems Technology*, 15(5):802–823, 2007.

[3] D. Habineza et al. Multivariable compensation of hysteresis, creep, badly damped vibration, and cross couplings in multiaxes piezoelectric actuators. *IEEE Trans Autom Sciences and Eng.*, 15:1639–1653, 2017.

[4] M. Al Janaideh, M. Al Saaideh, and M. Rakotondrabe. On hysteresis modeling of a piezoelectric precise positioning system under variable temperature. *MMSP*, 9:106880, 2020.

[5] G. Flores and M. Rakotondrabe. Robust nonlinear control for a piezoelectric actuator in a robotic hand using only position measurements. *IEEE Control Systems Letters*, 6:872–877, 2022.

[6] G. Flores et al. Model predictive control based on the generalized bouc-wen model for piezoelectric actuators in robotic hand with only position measurements. *IEEE Control Systems Letters*, 6:2186–2191, 2022.

[7] G. Flores and M. Rakotondrabe. Finite-time stabilization of the generalized bouc-wen model for piezoelectric systems. *IEEE Control Systems Letters*, 7:97–102, 2022.

[8] Gerardo Flores, V. González-Huitron, and A. E. Rodríguez-Mata. Output Feedback Control for a Quadrotor Aircraft Using an Adaptive High Gain Observer. *International Journal of Control, Automation and Systems*, 18(6):1474–1486, June 2020.

[9] Alejandro Flores and Gerardo Flores. Implementation of a Neural Network for Nonlinearities Estimation in a Tail-Sitter Aircraft. *Journal of Intelligent & Robotic Systems*, 103(2):22, September 2021.

[10] M. Rakotondrabe. Bouc–wen modeling and inverse multiplicative structure to compensate hysteresis nonlinearity in piezoelectric actuators. *IEEE Trans on Autom Science and Eng*, 8:428–431, 2011.

[11] R. Ballas. *Piezoelectric Multilayer Beam Bending Actuators*. 2007.

[12] G. Besançon. *Nonlinear observers and applications*, volume 363. Springer, 2007.

[13] Mohammad Reza-Rahmati and Gerardo Flores. A nonlinear observer for bilinear systems in block form. *European Journal of Control*, 70:100780, 2023.

[14] A. Rodríguez, G. Flores, A. Martínez, Z. Mora, R. Castro-Linares, and L. Amabilis. Discontinuous High-Gain Observer in a Robust Control UAV Quadrotor: Real-Time Application for Watershed Monitoring. *Mathematical Problems in Engineering*, 2018:4940360, November 2018. Publisher: Hindawi.

[15] A. Atassi et al. A separation principle for the control of a class of nonlinear systems. In *Proceedings of the 37th IEEE Conference on Decision and Control (Cat. No. 98CH36171)*, volume 1, pages 855–860, 1998.

[16] Gerardo Flores and Micky Rakotondrabe. Output feedback control for a nonlinear optical interferometry system. *IEEE Control Systems Letters*, 5(6):1880–1885, 2021.

[17] D. Costarelli et al. Constructive approximation by superposition of sigmoidal functions. *Anal. Theory Appl*, 29(2):169–196, 2013.

[18] F. Abdollahi et al. A stable neural network-based observer with application to flexible-joint manipulators. *IEEE Trans on Neural Networks*, 17(1), 2006.